

This is the accepted manuscript made available via CHORUS. The article has been published as:

Constraining Quirky Tracks with Conventional Searches

Marco Farina and Matthew Low

Phys. Rev. Lett. **119**, 111801 — Published 14 September 2017

DOI: [10.1103/PhysRevLett.119.111801](https://doi.org/10.1103/PhysRevLett.119.111801)

Constraining Quirky Tracks with Conventional Searches

Marco Farina*

*New High Energy Theory Center, Department of Physics, Rutgers University,
136 Frelinghuysen Road, Piscataway, NJ 08854, USA*

Matthew Low†

*School of Natural Sciences, Institute for Advanced Study,
Einstein Drive, Princeton, NJ 08540, USA*

Quirks are particles that are both charged under the standard model and under a new confining group. The quirk setup assumes there are no light flavors of the new confining group so that while the theory is in a confining phase, the quirk-antiquirk distance can be macroscopic. In this work, we reinterpret existing collider limits, those from monojet and heavy stable charged particle searches, as limits on quirks. Additionally, we propose a new search in the magnetic-field-less CMS data for quirks and estimate the sensitivity. We focus on the region where the confinement scale is roughly between 1 eV and 100 eV and find mass constraints in the TeV-range, depending on the quirk’s quantum numbers.

Introduction — The Large Hadron Collider (LHC) has now been running for several years and continues to be our most direct probe of electroweak-scale physics. The primary directions of phenomenological studies have been naturalness-driven and signature-driven. Along the signature-driven direction, only relatively small developments have been made in the study of unusual particle tracks. Track reconstruction at colliders relies on the simple assumption that all particles follow simple helical trajectories characteristic of the motion of charged particles in a magnetic field. There are new physics scenarios, however, that transcend that assumption and give rise to much stranger types of tracks at the LHC. Some examples of these track signatures include tracks that abruptly change direction (kinked tracks), tracks that begin part-way through the detector (appearing tracks), tracks with anomalous deposits of energy, and tracks with unusual curvature (see [1–8] for past and related theory studies). The latter case is typical of quirks, which will be the focus of this work.

Quirks are particles that are both charged under the standard model (SM) and under a new confining group [9–11]. The confinement scale is set by the running of the gauge coupling which is approximately logarithmic with energy such that an exponentially large range of confinement scales are reasonable. The quirk setup assumes there are no light flavors of the new confining group so that while the theory is in a confining phase, the quirk-antiquirk distance can be macroscopic. This leads to an interesting array of collider signatures based on the length, ℓ , of the flux tube, or string, between the quirk and antiquirk.

It is when ℓ becomes comparable to the length scales relevant for detectors that quirk tracks exhibit unusual curvature. Due to the challenges in identifying such tracks, there have been very few dedicated searches performed for quirks. A search from DZero sets the only bound on quirks which is $m_Q \gtrsim 120$ GeV when

$10 \text{ nm} \lesssim \ell \lesssim 100 \text{ } \mu\text{m}$ (where the individual quirks are not resolved) [12].

In this work, we will show for the first time that strong bounds can be set on quirks, at collider-relevant scales, using entirely standard LHC searches with no modifications to tracking algorithms. These searches are sensitive for macroscopic string lengths. In addition to reinterpreting existing searches, we propose a new search that can be performed in the magnetic-field-less “0T” data of CMS (still using standard tracking algorithms). In the 0T data all known electrically charged particles are expected to leave straight tracks making this dataset a nearly background-free sample for certain types of tracks with anomalous curvature. While we propose a specific search for quirks, we are optimistic that the use of such a dataset can be extended to other scenarios beyond quirks.

Quirks (at the LHC) — We now introduce the minimal ingredients for a quirk model. To the SM gauge group we add a new “infracolor” gauge group that is assumed to be asymptotically-free with a confinement scale Λ and to the SM particle content we add a new species, Q , with mass m_Q and infracolor representation size N_c . The particle Q is called a quirk when it is much heavier than the confinement scale ($m_Q \gg \Lambda$). Since Q is assumed to be the lightest infracolored particle, there are no particles lighter than Λ that can form “hadrons” and the only hadronic states are glueballs with masses a little above Λ . When a quirk and antiquirk are produced, for instance at the LHC, there are no light hadrons to break the infracolor flux tube between the quirks. This flux tube, or string, connecting the quirk and antiquirk can be macroscopic in size and its tension results in an attractive force between the two particles.

We can now study the trajectory of quirks at the LHC. The equations of motion are given by the Nambu-Goto action with point masses on the ends of the string in an

electromagnetic background [11, 13]. For a single quirk, the equation of motion is

$$\frac{\partial}{\partial t} (m_Q \gamma \vec{v}) = -T \sqrt{1 - \vec{v}_\perp^2} \left(\hat{s} - \frac{v_\parallel \vec{v}_\perp}{1 - \vec{v}_\perp^2} \right) + q \vec{v} \times \vec{B}. \quad (1)$$

Above \hat{s} is a unit vector that points towards the other quirk and is used to define $v_\parallel = (\vec{v} \cdot \hat{s})$, $\vec{v}_\parallel = v_\parallel \hat{s}$, and $\vec{v}_\perp = \vec{v} - \vec{v}_\parallel$. The quirk mass is m_Q , the quirk **electric** charge is q , and the magnetic field is \vec{B} . For both the HSCP and monojet searches we use the CMS magnetic field of $\vec{B} = (0, 0, 3.8 \text{ T})$ while for the 0T search we use $\vec{B} = 0$. The tension is given by T which is proportional to Λ^2 . There have been estimates that $T \simeq 1.6 \Lambda^2$ in QCD [14], but we take $T = \Lambda^2$ for simplicity (as the difference is simply a rescaling of the parameter space).

In the absence of external forces and when the quirks are back-to-back the maximum distance between them can be calculated to be

$$\ell_{\text{eff}} = \frac{2m_Q}{\Lambda^2} (\gamma - 1) = \frac{m_Q}{\Lambda^2} v^2 + \mathcal{O}(v^4), \quad (2)$$

where γ is the boost factor. While the true string length, ℓ , can be different, we use ℓ_{eff} as a simple approximation. The m_Q/Λ^2 factor follows from dimensional analysis and the v^2 factor plays a relevant role in collider searches. Numerically, one has

$$\ell_{\text{eff}} \approx 10 \text{ m} \left(\frac{m_Q}{1 \text{ TeV}} \right) \left(\frac{100 \text{ eV}}{\Lambda} \right)^2 \left(\frac{v}{0.7} \right)^2. \quad (3)$$

From Eq. (3) one can map different types of searches to the appropriate range of Λ . For $10 \text{ keV} \lesssim \Lambda \lesssim 1 \text{ MeV}$ the quirks only separate a microscopic distance, comparable to the typical tracking resolution ($\sim \mu\text{m}$) so that the quirk-antiquirk system is observed as a single highly-ionizing straight track [12]. For $1 \text{ eV} \lesssim \Lambda \lesssim 10 \text{ keV}$ one finds that ℓ_{eff} is macroscopic and leads, in general, to oddly curved tracks. Finally, for $\Lambda \lesssim 1 \text{ eV}$ the effective string length is megascopic and does not play a role in collider searches, leaving the quirks to appear as heavy stable charged particles (HSCP).

Reinterpreting Existing Searches — As mentioned above, for a wide range of Λ there is a non-zero probability that a quirk track would be reconstructed at the LHC. When this happens the quirk will appear simply as a heavy stable (or long-lived) charged particle. In a collider, such particles are found by looking for tracks with large deposits of energy and/or a long time of flight (as compared to muons). When both tracks fail to be reconstructed monojet searches will have sensitivity, provided that the quirks have been produced in association with a sufficiently energetic jet (through either initial or final state radiation). Monojet searches look for large missing transverse energy that results from a jet recoiling against undetected particles.

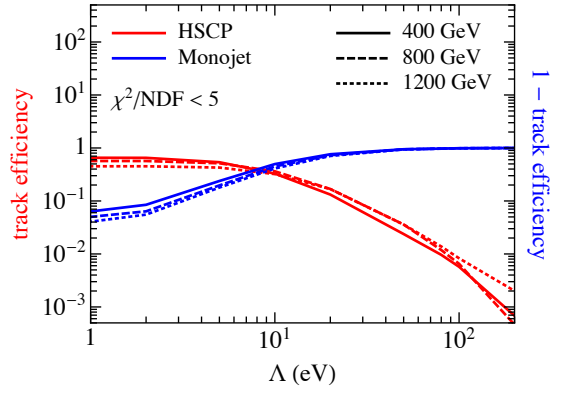


FIG. 1: Track efficiency as a function of confinement scale, Λ , for various quirk masses with a magnetic field of $\vec{B} = (0, 0, 3.8 \text{ T})$ at 13 TeV for HSCP events (red) and monojet events (blue). The efficiencies do not asymptote to 0 or 1 at small Λ due to the other track cuts applied (see Table I).

The probability to reconstruct a track is characterized by the track efficiency and is shown in Fig. 1 for HSCP searches (red) and for monojet searches (blue). The track efficiency is computed by applying a series of track selection cuts (as used by CMS in their HSCP analysis [15]) listed in Table I and described below.

First, the quirk propagation is found by solving the equations of motion. We use the straight string approximation throughout. Each time a quirk passes through a tracker layer it registers as a hit with an efficiency that we assume to be 100%. To account for the fact that in practice the hit efficiency is $\gtrsim 95\%$ [16] we increase the minimum number of layers a track must hit, n_{hits} , requirement to ≥ 9 from the typical ≥ 8 as a conservative measure.

We model the tracker geometry following the specifications of the CMS tracker,¹ which consists of a combination of barrel layers and endcap layers that cover the range $-2.5 < \eta < 2.5$ where a particle will pass through $\approx 11 - 16$ layers depending on its trajectory [17].

The tracks are then fit to a helix, which corresponds to the trajectory of an electrically charged particle in the longitudinal magnetic field of the detector. A helix is given by

$$h_x(t; R, \phi, \lambda) = R \cos(\phi \pm (t/R) \cos \lambda) - \cos \phi, \quad (4a)$$

$$h_y(t; R, \phi, \lambda) = R \sin(\phi \pm (t/R) \cos \lambda) - \sin \phi, \quad (4b)$$

$$h_z(t; R, \phi, \lambda) = t \sin \lambda, \quad (4c)$$

where t is the parameter along the curve, R is the radius, ϕ is the initial azimuthal direction, and λ is the dip angle.

¹ We use the CMS tracker to maximize the accuracy of our results for the HSCP and 0T searches.

cut	HSCP	monojet	0T
$ \eta $	< 2.1	< 2.5	< 2.1
n_{hits}	≥ 9	≥ 9	≥ 9
v	> 0.6	—	—
p_T^{eff}	$> 65 \text{ GeV}$	$> 10 \text{ GeV}$	$> 65 \text{ GeV}$
χ^2/NDF	< 5	< 5	< 5
R	—	—	$< 1500 \text{ m}$

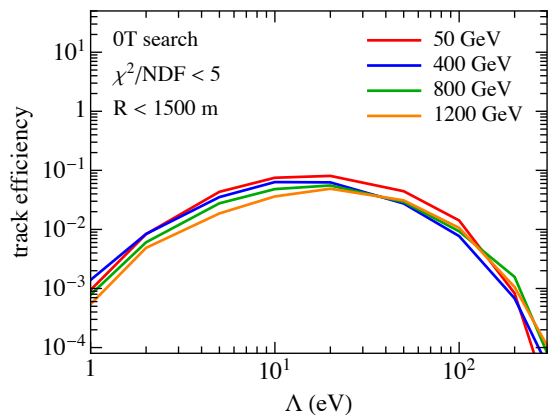
TABLE I: Cut flow for identifying a track.

For a completely general helix there are 3 additional parameters specifying the initial position of the helix, but we set this to the origin.² The \pm depends on the charge of the particle.

Next, we perform a χ^2/NDF fit to Eq. (4) and assume that quirks with $\chi^2/\text{NDF} < 5$ would be reconstructed as tracks [15]. We use a spatial resolution of $30 \mu\text{m}$ for each hit [17]. The p_T^{eff} cut is applied to the measured p_T of the track (computed from the best fit R value) rather than the true p_T of the particle.

The first search that we reinterpret is the HSCP search. The most sensitive HSCP searches have been performed at 13 TeV by CMS with 12.9 fb^{-1} [15] and by ATLAS with 3.2 fb^{-1} [18] and are presented as mass limits on stable particles of different SM charges. We follow the event selection of the former analysis which primarily consists of a χ^2/NDF cut on the track and a cut of $p_T^{\text{eff}} > 65 \text{ GeV}$. We only consider the sample that would be selected by the muon trigger which adds the additional requirement that $v > 0.6$ in order that the trigger be $\approx 100\%$ efficient. We generate quirk-antiquirk events using Madgraph 5 v2.3.3 [19]. The tracking efficiency is shown in Fig. 1 (red). We define the track efficiency as the number of tracks passing all track requirements divided by the number of tracks passing the $|\eta|$ cut.

The second search we reinterpret is the monojet search. From CMS the strongest search is at 13 TeV and uses 12.9 fb^{-1} [20] and from ATLAS it is at 13 TeV using 3.2 fb^{-1} [21]. While the CMS search has better reach, we use the ATLAS limits because they are presented as limits on compressed stop squarks which is kinematically more similar to quirk events than the setups in the CMS search. We also show limits scaling the ATLAS result up to 12.9 fb^{-1} . We generate quirk-antiquirk events along with a radiated jet of $p_T > 200 \text{ GeV}$ and follow the monojet event selection in [21]. The track selection in this case still identifies when a good track would be selected, however, opposite to the HSCP case, this means the event would be rejected. For this reason we plot the quantity $(1 - \text{track efficiency})$ in Fig. 1 (blue).

FIG. 2: Track efficiency as a function of confinement scale, Λ , for various quirk masses with a magnetic field of $\vec{B} = 0$ at 13 TeV.

Using the 0T Data — In addition to the reinterpreted searches, we propose an entirely new search whose sensitivity is maximal in the challenging region near $\Lambda \sim 10 \text{ eV}$. This search makes use of the 0.6 fb^{-1} of 13 TeV data with a 0T magnetic field [22]. Without a magnetic field, all SM particles, both electrically neutral and charged, travel in straight lines. Quirks, on the other hand, still curve due to the string tension. This means one can simply count the number of curved tracks in the 0T data and accordingly set a limit or make an observation of quirks. Operationally, this would entail running the tracking algorithm on the 0T data while pretending there is a magnetic field and should not require any modifications to the tracking algorithm itself.

The efficiency for identifying a track in the 0T data is shown in Fig. 2. For the 0T search we use the monojet trigger [23] which uses an analysis-level cut of $p_T > 100 \text{ GeV}$ for the leading jet and $\cancel{E}_T > 200 \text{ GeV}$ where \cancel{E}_T excludes muons (and would also exclude the quirk tracks). While in principle one could use the muon trigger as in done in the HSCP searches, in practice the monojet trigger is more effective. The reason is that without sizable initial radiation for the quirk system to recoil against, the quirks will be almost back-to-back in the transverse plane. This means there is no curvature in the xy -plane so that the quirk trajectories cannot be reconstructed as non-straight helices. Therefore, at least some initial state radiation is required for a non-zero efficiency.

We generate events with a single jet with $p_T > 200 \text{ GeV}$ and apply the track cuts in Table I. These closely follow the selection from the HSCP search with the exception that we add a requirement that the fitted radius must be $R < 1500 \text{ m}$. We estimate the R value from the sagitta s of a track

$$s \approx \frac{d_{\text{max}}^2}{8R}, \quad (5)$$

² Our results are not sensitive to this assumption.

where d_{\max} is the chord length, corresponding to the radius of the tracker. We take $d_{\max} \approx 1$ m [17] and set the sagitta to the single hit resolution of $s \approx 30 \mu\text{m}$ [17]. A straight 3-hit track with a 3σ fluctuation in the sagitta of a single hit gives $R \approx 1500$ m. Since a straight track faking a quirk requires ≥ 9 hits, the fake rate is much lower than indicated by the 3σ requirement. The R cut is responsible for the decrease in track efficiency at $\Lambda < 20$ eV.

We assume that the fake rate is sufficiently low and that multiple scattering effects faking a curved track are sufficiently rare to treat the analysis as zero-background. In principle, if a track with non-zero curvature is discovered the event could be inspected and checked for the presence of a second curved track, providing a smoking gun of the signal. A limit is projected corresponding to observing ≤ 3 events [24].

Discussion of Results — The results are shown, for a $(\mathbf{3}, \mathbf{1})_{2/3}$ fermion with $N_c = 2$, in Fig. 3. The shaded red region shows the limits from HSCP searches which drive the limits for $\Lambda \lesssim 200$ eV. The shaded green region shows the limits from the ATLAS monojet search that used 3.2 fb^{-1} and the unshaded green dashed line scales up the limit to a projected luminosity of 12.9 fb^{-1} (the amount used in the CMS monojet search). Our projection for the 0T search is given by the shaded blue region which uses 0.6 fb^{-1} . The dashed blue line shows a hypothetical dataset of 20 fb^{-1} with no magnetic field and is the minimum amount of data required to be competitive with HSCP and monojet searches. The HSCP and 0T bounds are cut off at $\Lambda = 300$ eV because our statistics there are insufficient for a reliable estimate.

Regarding QCD hadronization, the HSCP searches at the LHC use two different models [15, 18]. The first model [25, 26] assumes that the heavy hadrons can be electrically charged or neutral when exiting the calorimeter while the second model [27] assumes the all heavy hadrons are neutral when exiting the calorimeter. The 0T search only uses information from the tracker and therefore does not depend on this assumption. We take the fraction of R -hadrons that are charged to be 0.55 from Pythia 8 [28].

For the 0T and HSCP searches we allow for 1 or 2 identified tracks while for the monojet search we require 0 identified tracks. The overall efficiency includes an acceptance factor ($\approx 85 - 95\%$ in the relevant region) that was not used in Figs. 1 and 2.

In Table II we report the limits for various other quantum numbers using $\Lambda = 1$ eV, $\Lambda = 100$ eV, and $\Lambda = 10^3$ eV as benchmark points.

The gray lines in Fig. 3 show contours of constant ℓ_{eff} . The v used to compute ℓ_{eff} is the mean of the velocity distribution at 13 TeV. The ℓ_{eff} contours give an idea of the length scales where each search is most effective and conversely, show where in parameter space other types of

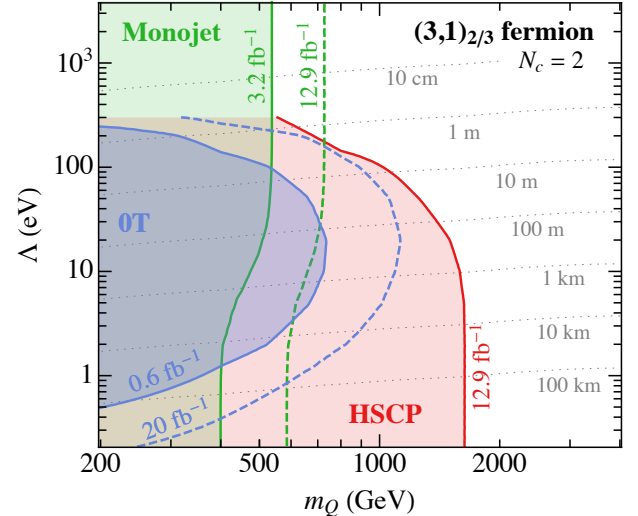


FIG. 3: The 95% C.L. limits on a color triplet fermionic quirk with $N_c = 2$. The red/green bound comes from HSCP/monojet searches and the blue bound is our projection for the 0T data. Colored dashed lines correspond to future luminosity projections. The grey dotted lines show contours of ℓ_{eff} .

spin	SM charge	N_c	m_Q ($\Lambda = 1$ eV)	m_Q ($\Lambda = 100$ eV)	m_Q ($\Lambda = 10^3$ eV)
fermion	$(\mathbf{3}, \mathbf{1})_{2/3}$	2	1.6 TeV	1.0 TeV	500 GeV
scalar	$(\mathbf{3}, \mathbf{1})_{2/3}$	2	1.3 TeV	700 GeV	350 GeV
fermion	$(\mathbf{1}, \mathbf{1})_{-1}$	2	650 GeV	150 GeV	—
scalar	$(\mathbf{1}, \mathbf{1})_{-1}$	2	350 GeV	60 GeV	—
fermion	$(\mathbf{3}, \mathbf{1})_{2/3}$	5	1.8 TeV	1.1 TeV	600 GeV
scalar	$(\mathbf{3}, \mathbf{1})_{2/3}$	5	1.4 TeV	850 GeV	450 GeV
fermion	$(\mathbf{1}, \mathbf{1})_{-1}$	5	800 GeV	200 GeV	30 GeV
scalar	$(\mathbf{1}, \mathbf{1})_{-1}$	5	450 GeV	80 GeV	—

TABLE II: Quirk mass limits for various quantum numbers at the benchmark points of $\Lambda = 1$ eV, $\Lambda = 100$ eV, and $\Lambda = 10^3$ eV. N_c is the infracolor representation size.

quirk searches would lie.

For $\Lambda \lesssim 1$ eV, smaller than shown in Fig. 3, the 0T limit quickly goes away but the HSCP limit stays constant at 1.6 TeV because ℓ_{eff} simply gets larger. On the other end, for $\Lambda \gtrsim 200$ eV, the monojet limit stays constant until $\ell_{\text{eff}} \sim \mu\text{m}$ where the quirk system will appear as a single straight track. Here, HSCP searches might have some sensitivity again.

Outlook — In this paper, we demonstrated that while quirk dynamics can result in very exotic tracks, they can also result in very standard looking tracks allowing for

standard searches to constrain a substantial region of parameter space. In particular, reinterpreting HSCP and monojet searches allows one to set limits in the regions $\Lambda \lesssim 100$ eV ($\ell_{\text{eff}} \gtrsim 1$ m) and $\Lambda \gtrsim 1$ eV ($\ell \lesssim 100$ km) respectively.

We then proposed a novel use of the 0T data from CMS which involved looking for curved tracks in the dataset. Amusingly, the 0T search could outdo the current HSCP limits if it had only $\gtrsim 20$ fb $^{-1}$ of data.

We chose a few sample quantum numbers, in Table II, but it would be interesting to see limits for a larger variety of quantum numbers. On the experimental side, it would be interesting to see if dedicated quirk searches can be done and would they compare to the monojet and HSCP searches.

Finally, given the simplicity of our 0T analysis, we

hope that this work can serve as motivation for moving towards more involved tracking modifications in order to fully exploit the LHC's potential for unusual tracks.

The authors would like to thank Raffaele Tito D'Agnolo, Markus Luty, Duccio Pappadopulo, Joshua Ruderman, Andreas Salzburg, and Kris Sigurdson for useful discussions and Yuri Gershtein, Philip Harris, Simon Knapen, Scott Thomas, and Nhan Tran for helpful discussions and reading the manuscript. M.F. is supported in part by the DOE Grant DE-SC0010008. M.L. is supported by a Frank and Peggy Taplin membership at the Institute for Advanced Study. This work was partly completed at KITP, which is supported in part by the National Science Foundation under Grant No. NSF PHY11-25915 and at the Aspen Center for Physics, which is supported by National Science Foundation grant PHY-1066293.

* farina.phys@gmail.com

† mattlow@ias.edu

- [1] G. Burdman, Z. Chacko, H.-S. Goh, R. Harnik, and C. A. Krenke, *Phys. Rev.* **D78**, 075028 (2008), [arXiv:0805.4667 \[hep-ph\]](#).
- [2] R. Harnik and T. Wizansky, *Phys. Rev.* **D80**, 075015 (2009), [arXiv:0810.3948 \[hep-ph\]](#).
- [3] S. Asai, Y. Azuma, M. Endo, K. Hamaguchi, and S. Iwamoto, *JHEP* **12**, 041 (2011), [arXiv:1103.1881 \[hep-ph\]](#).
- [4] R. Harnik, G. D. Kribs, and A. Martin, *Phys. Rev.* **D84**, 035029 (2011), [arXiv:1106.2569 \[hep-ph\]](#).
- [5] P. Meade, M. Papucci, and T. Volansky, *Phys. Rev. Lett.* **109**, 031801 (2012), [arXiv:1103.3016 \[hep-ph\]](#).
- [6] R. Fok and G. D. Kribs, *Phys. Rev.* **D84**, 035001 (2011), [arXiv:1106.3101 \[hep-ph\]](#).
- [7] S. Jung and H.-S. Lee, (2015), [arXiv:1503.00414 \[hep-ph\]](#).
- [8] S. Knapen, S. Pagan Griso, M. Papucci, and D. J. Robinson, (2016), [arXiv:1612.00850 \[hep-ph\]](#).
- [9] L. B. Okun, *JETP Lett.* **31**, 144 (1980), [*Pisma Zh. Eksp. Teor. Fiz.* 31,156(1979)].
- [10] L. B. Okun, *Nucl. Phys.* **B173**, 1 (1980).
- [11] J. Kang and M. A. Luty, *JHEP* **11**, 065 (2009), [arXiv:0805.4642 \[hep-ph\]](#).
- [12] V. M. Abazov et al. (D0), *Phys. Rev. Lett.* **105**, 211803 (2010), [arXiv:1008.3547 \[hep-ex\]](#).
- [13] M. Luscher and P. Weisz, *JHEP* **07**, 049 (2002), [arXiv:hep-lat/0207003 \[hep-lat\]](#).
- [14] A. Deur, S. J. Brodsky, and G. F. de Teramond, *Phys. Lett.* **B750**, 528 (2015), [arXiv:1409.5488 \[hep-ph\]](#).
- [15] [Search for heavy stable charged particles with 12.9 fb \$^{-1}\$ of 2016 data](#), Tech. Rep. CMS-PAS-EXO-16-036 (CERN, Geneva, 2016).
- [16] V. Khachatryan et al. (CMS), *Eur. Phys. J.* **C70**, 1165 (2010), [arXiv:1007.1988 \[physics.ins-det\]](#).
- [17] S. Chatrchyan et al. (CMS), *JINST* **3**, S08004 (2008).
- [18] M. Aaboud et al. (ATLAS), *Phys. Lett.* **B760**, 647 (2016), [arXiv:1606.05129 \[hep-ex\]](#).
- [19] J. Alwall, R. Frederix, S. Frixione, V. Hirschi, F. Maltoni, O. Mattelaer, H. S. Shao, T. Stelzer, P. Torrielli, and M. Zaro, *JHEP* **07**, 079 (2014), [arXiv:1405.0301 \[hep-ph\]](#).
- [20] [Search for dark matter in final states with an energetic jet, or a hadronically decaying W or Z boson using 12.9 fb \$^{-1}\$ of data at \$\sqrt{s} = 13\$ TeV](#), Tech. Rep. CMS-PAS-EXO-16-037 (CERN, Geneva, 2016).
- [21] M. Aaboud et al. (ATLAS), (2016), [arXiv:1604.07773 \[hep-ex\]](#).
- [22] V. Khachatryan et al. (CMS), *Phys. Rev. Lett.* **117**, 051802 (2016), [arXiv:1606.04093 \[hep-ex\]](#).
- [23] [Search for dark matter production in association with jets, or hadronically decaying W or Z boson at \$\sqrt{s} = 13\$ TeV](#), Tech. Rep. CMS-PAS-EXO-16-013 (CERN, Geneva, 2016).
- [24] G. J. Feldman and R. D. Cousins, *Phys. Rev.* **D57**, 3873 (1998), [arXiv:physics/9711021 \[physics.data-an\]](#).
- [25] A. C. Kraan, *Eur. Phys. J.* **C37**, 91 (2004), [arXiv:hep-ex/0404001 \[hep-ex\]](#).
- [26] R. Mackeprang and A. Rizzi, *Eur. Phys. J.* **C50**, 353 (2007), [arXiv:hep-ph/0612161 \[hep-ph\]](#).
- [27] R. Mackeprang and D. Milstead, *Eur. Phys. J.* **C66**, 493 (2010), [arXiv:0908.1868 \[hep-ph\]](#).
- [28] T. Sjstrand, S. Ask, J. R. Christiansen, R. Corke, N. Desai, P. Ilten, S. Mrenna, S. Prestel, C. O. Rasmussen, and P. Z. Skands, *Comput. Phys. Commun.* **191**, 159 (2015), [arXiv:1410.3012 \[hep-ph\]](#).